Proceedings of the 28th IEEE
EMBS Annual International Conference
New York City, USA, Aug 30-Sept 3, 2006

Detection of murine infarcts using myocardial elastography at both high temporal and spatial resolution

Jianwen Luo, *Member, IEEE*, Kana Fujikura, and Elisa E. Konofagou, *Associate Member, IEEE*

***Abstract*—Myocardial elastography is a novel method for noninvasively assessing regional myocardial function, with the advantages of high spatial/temporal resolution, high signal-to-noise ratio and angle-independence. In this paper, *in vivo* experiments were performed in anesthetized normal and infarcted mice using a high-resolution ultrasound system. Radio-frequency signals were acquired at a high frame rate (up to 8000 Hz) and used to estimate the incremental axial displacements and strains of myocardium. The incremental results were further used to calculate the cumulative displacements and strains. Two-dimensional displacement and strain images (elastograms), M-mode displacement and strain images as well as displacement and strain profiles as a function of time clearly indicated the contraction and relaxation, thickening and thinning of myocardium and demonstrated the lower motion and deformation of infarcted myocardium. The cumulative displacement and strain were less noisy than incremental images, and the cumulative strain images show the highest contrast between non-infarcted and infarcted myocardia. Finally, preliminary statistical results from nine non-infarcted mice and seven infarcted mice indicated that cumulative strain can be used to differentiate infarcted myocardium from non-infarcted myocardium. In conclusion, myocardial elastography can provide strain information at both high temporal and spatial resolution, and is capable of accurately characterizing normal myocardial function as well as detecting and localizing early myocardial infarction *in vivo*.**

I. Introduction

The non-invasive estimation of regional myocardial function plays a crucial role in clinical cardiology. Echocardiography is the predominant imaging modality in diagnostic cardiology because it is portable, readily available and real-time. More specifically, stress echocardiography [1] can assess regional wall motion and thickening. However, this approach is only qualitative or semi-quantitative and heavily depends on the operator experience and expertise. Tissue Doppler imaging (TDI) or Doppler myocardial imaging (DMI) [2] and strain rate imaging (SRI) [3] use Doppler-based techniques to obtain regional velocity estimates and velocity gradients (i.e., strain rate). However, Doppler-based methods use small bandwidth signal and therefore have the disadvantages of low axial resolution. In addition, these methods are angle-dependent because only one-dimensional information in the axial direction of ultrasound probe can be provided whereas hearts undergo complicated motions including translation, rotation, expansion, contraction, and shear in three-dimensional space. In addition to the echocardiography-based techniques, magnetic resonance (MR) cardiac tagging [4] has also been shown capable of estimating three-dimensional strain tensors with high precision, but at the cost of low spatial resolution limited by the tag spacing, low temporal resolution and long examination times. In addition, MRI equipment can be non-portable and costly.

Ultrasound elastography [5] has been developed into a successful approach for estimating and imaging the local strain in tissues which undergo internal or external, static or quasi-static compression. The axial displacements within tissues are firstly estimated from the radio-frequency (RF) signals or B-mode images before and after compression, normally using the cross-correlation function, sum of absolute difference (SAD) or sum of square difference (SSD) techniques. The axial strains are then calculated using the spatial derivative (gradient) of the axial displacements. The axial strains are related to mechanical properties of tissues, e.g., Young's modulus or shear modulus. Therefore ultrasound elastography is capable of providing the information of mechanical property distribution within tissues which conventional medical imaging modalities cannot provide directly.

Myocardial elastography utilizes the inherent cardiac muscle function as the mechanical stimulus and acquires successive data frames to estimate the displacements and strains of the myocardium [6]. Similar technique has previously been validated in a tissue-mimicking phantom [7] and also shown to be feasible in imaging the motion of healthy human myocardium [8] using speckle tracking. A preliminary comparison study of infarcted (ischemic) myocardium and non-infarcted (normal) myocardium was also performed and results showed the infarcted regions could be identified and differentiated from the non-infarcted ones [9]. However, this study employed envelope-detected (B-mode) data to estimate the axial displacements and hence has lower precision and resolution compared to the use of RF signals. Another comparison study also indicated that myocardial elastography could offer comparable quality estimates to those obtained with MR cardiac tagging; with the added advantage of higher temporal and spatial resolution [10]. In addition to axial displacements and strains,

Manuscript received April 24, 2006. This work was supported in part by the American Heart Association under Grant 0435444AT.

J. Luo, K. Fujikura, and E. E. Konofagou are with are with the department of biomedical engineering of Columbia University, New York, NY 10027, USA (e-mail: jl2767@columbia.edu, kf2113@columbia.edu, and ek2191@columbia.edu, respectively).

myocardial elastography can obtain lateral displacements and strains [6], [11]. By combining the two components of the strain tensors calculated from the two-dimensional displacements, the radial / circumferential / principal strains can be calculated as angle-independent measurements of the myocardial function [12].

II. Methods

Nine wild-type mice were anesthetized with 125 mg/kg intraperitoneal injection of tribromoethanol. The hair was removed using potassium thioglycolate and the mouse was placed in supine position on a heating platform (VisualSonics Inc., Toronto, Ontario, Canada) in order to keep the body temperature steady. ECG signal was obtained from the electrode pads on the mouse platform. Ultrasound probe was placed on the chest using degassed ultrasound gel (Aquasonic 100, Parker Laboratories, Inc., Orange, Fairfield, NJ) as a coupling medium. After the mice were scanned, myocardial infarction (MI) was induced by permanent ligation of the left anterior descending coronary artery (LAD) in mice after left sided thoracotomy. Two mice died during the operation while the remaining mice (MI mice) were scanned one day after the operation.

A high-resolution imaging system specially developed for small animal research (VisualSonics Vevo 770, VisualSonics Inc., Toronto, Ontario, Canada) was used for this study. The high-frequency ultrasound probe (RMV-707) was composed of a fixed-focused transducer working at 30 MHz, with a focal depth of 12 mm. The transducer was mechanically rotated and real-time 2D images were acquired at a frame rate up to 60 Hz. The field of view is 12 mm × 12 mm, the axial resolution is 50 μm, and the lateral resolution 100 μm. The ultrasound probe was placed on the chest in the parasternal position to obtain a longitudinal (low axis) view of the left ventricle of the heart.

A two-channel, 200 MS/s, 14 Bit Waveform Digitizer for PCI Bus (CompuScope 14200, Gage Applied Technologies, Inc., Lachine, QC, Canada) was used to synchronously acquire the radio-frequency (RF) signal of the ultrasound scanner and the electrocardiogram (ECG) signal.

In addition to the real-time scanning mode (B-mode), an EKV (ECG-based kilohertz visualization) mode provided by the imaging system allows high frame rate acquisitions of the mouse heart. The ultrasound acquisition of each RF lines was triggered on the mouse ECG. The transducer was slowly rotated and ultrasound echo signals were recorded at a pulse-repetition frequency (PRF) of 8000 pulses/s at each position of the transducer. The ECG was recorded simultaneously and allows the triggering based on the R-wave peaks.

During our acquisition, the RF signals and ECG signals were digitized synchronously and transferred to the computer in real time. After the acquisition, the RF lines were aligned on the R-wave peaks. With such a technique similar to EKV reconstruction, the complete set of 2D ultrasound RF data was reconstructed at an extremely high frame rate of 8000 frames/s for a complete heart cycles [13].

The axial displacements of the tissue were estimated off-line using a speckle tracking method based on the cross-correlation calculation. The window size was 240 μm, while the window overlap was equal to 90%. To reduce the noise amplification effect of the gradient operation, a piecewise least-square estimator with a window size of 240 μm was used to calculate the axial strains.

After the incremental displacements and strains were estimated from every two consecutive RF frames, the results were further processed to obtain the cumulative displacements and strain, respectively. In this procedure, the automated tissue tracking was implemented according to the displacement estimation to make sure that the displacement and strain traces represent the same myocardial segment over the whole cardiac cycle.

III. RESULTS

Figure 1 shows the displacement images (a, c) and strain images (b, d) of a normal myocardium in the phases of systole (a, b) and diastole (c, d), respectively. The displacements and strains are color-coded and overlaid onto the grayscale ultrasound image. On the images, the displacements and strains of the myocardium are shown but those of the blood in the cavity are filtered out using a threshold on the speckle energy. The displacement images and elastograms are displayed in the scale of [-0.001 0.001] mm and [-0.1% 0.1%], respectively. The red points in the ECG signals below show the temporal positions of these images. In the displacement images, positive displacements (in red color) denotes motions toward the transducer (located at the top) and negative displacements (in blue color) away from the transducer. In the strain images, positive and negative values (in red and blue colors) represent tension (thickening) and compression (thinning) of myocardium, respectively.

In the systolic phase, as shown in (a), the myocardium contraction is clearly visible, with septum moving down and the lateral wall moving up. In the diastolic phase (b), displacements have opposite directions while the myocardium relaxes. On the strain images of the systolic phase (c), red strains are visible in the septum and posterior wall, indicating thickening of myocardium. And in the diastolic phase, the blue strains in the septum and posterior wall reflect the thinning of myocardium.

Figure 2 shows the displacement images (a, c) and elastograms (b, d) of an infarcted myocardium in the systolic phase (a, b) and diastolic phase (c, d), respectively. Similar to Fig. 1, Fig. 2 also shows the contraction and relaxation of myocardium, as well as the thickening and thinning of myocardium in the septum. Compared to results in Fig. 1, the displacements and strains in the septum in Fig. 2 are relatively smaller. Because of the attenuation of the high-frequency ultrasound, the posterior wall is hypoechoic in the grayscale ultrasound image and the amplitudes of corresponding RF signals are very low. Therefore, the sonographic

signal-to-noise ratio is lower and the estimated displacement and strain are noisier in the posterior wall than in the septum. The posterior wall may have a more complex motion, including the out-of-plane motion of the papillary muscle and the effect of the lung due to respiration. In addition, because the ischemic region is in the septum of the infarcted heart, we concentrate the results in the septum.

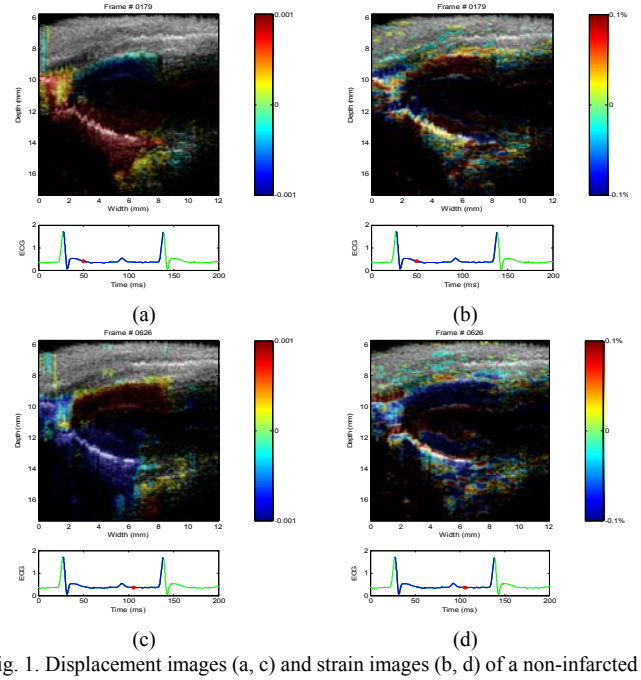

Fig. 1. Displacement images (a, c) and strain images (b, d) of a non-infarcted myocardium in the phases of systole (a, b) and diastole (c, d).

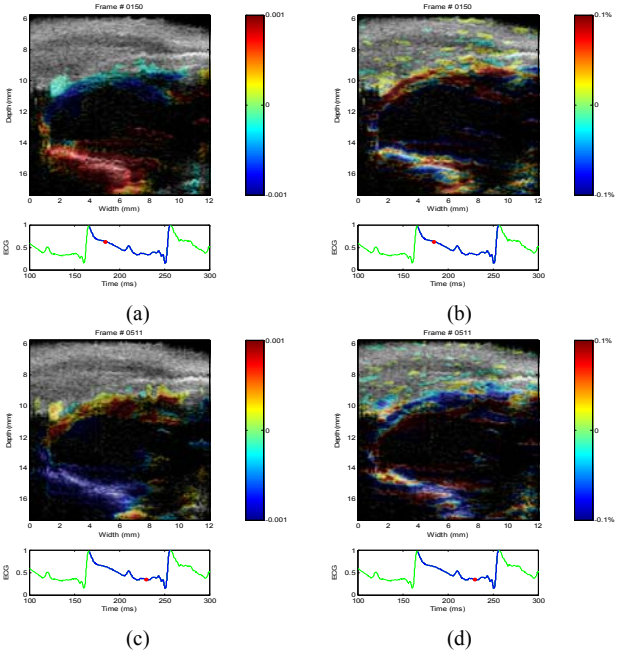

Fig. 2. Displacement images (a, c) and strain images (b, d) of an infarcted myocardium in the phases of systole (a, b) and diastole (c, d).

A temporal analysis of the displacements and strains was performed for individual RF lines of the images. Fig. 3 shows the color-coded incremental displacement, incremental strain, cumulative displacement and cumulative strain along the RF line at the lateral location of 5 mm of the non-infarcted myocardium, where the horizontal axis denotes time and vertical axis denotes depth. The incremental images show the contraction and thickening of myocardium (systole) that started on the R-wave peak of the ECG, followed by the relaxation and thinning (diastole). The cumulative images are much more smoothed than the incremental results. The cumulative displacement increases from 0 during the systolic phase and peaks at end systole, indicating the contraction of myocardium. During diastolic phase, the cumulative displacement decreases and returns to 0 at end diastole. Similarly, the cumulative strain is largest at end systole, which represents the total deformation during systole.

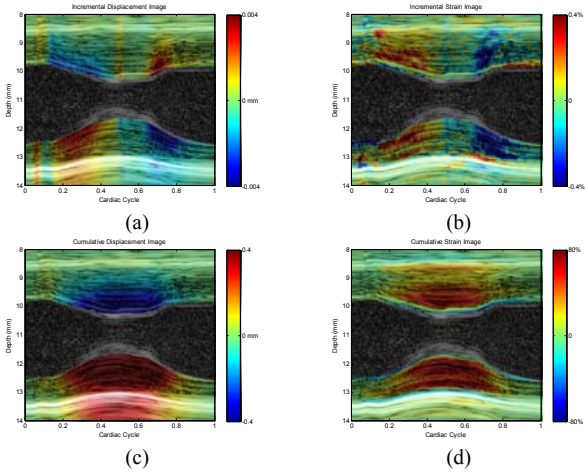

Fig. 3. Temporal variation of the incremental displacement (a), incremental strain (b), cumulative displacement (c) and cumulative strain (d) along the RF line at 5 mm of the non-infarcted myocardium

Figure 4 shows the incremental/cumulative displacement/strain along the RF line at 5 mm of the infarcted myocardium. The incremental displacement and strain in the septum are smaller that those of non-infarcted myocardium.

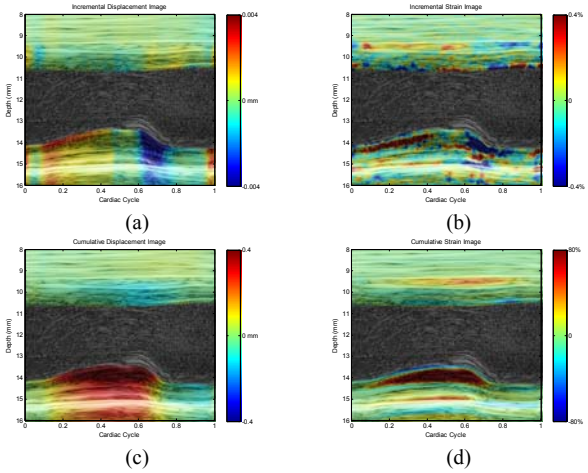

Fig.4. Temporal variation of the incremental displacement (a), incremental strain (b), cumulative displacement (c) and cumulative strain (d) along the RF line at 5 mm of the infarcted myocardium.

Figure 5 compares the displacement and strain variation with time of the non-infarcted and infarcted myocardia. The profiles were calculated from Figs. 3 and 4, by averaging over a small region in the septum where the displacements and strains are relatively uniform. Lower motion and deformation can be seen in the non-infarcted myocardium. The result also

shows the highest contrast in cumulative strain profiles between non-infarcted and infarcted myocardia, highlighting that the cumulative strain is more suitable in distinguishing infarcted from non-infarcted myocardium.

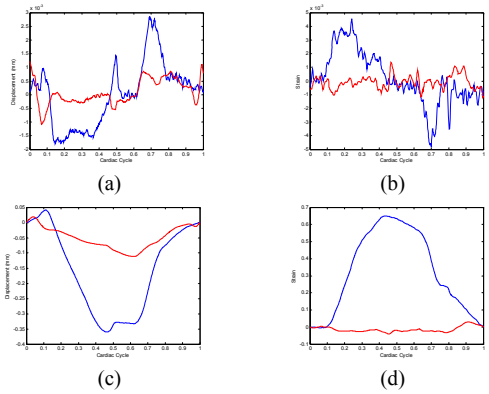

(a) (b) (c) (d)

Fig. 5. The incremental displacements (a), incremental strains (b), cumulative displacements (c) and cumulative strains (d) of the non-infarcted (blue) and infarcted (red) myocardia.

Figure 6 compares the cumulative elastograms of the non-infarcted and infarcted myocardia at end systole. The ischemic region is clearly detected with smaller strain compared to the normal region.

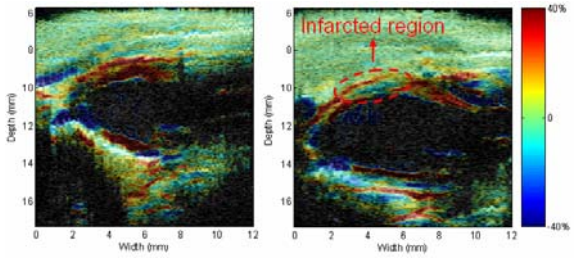

(a) (b)

Fig. 6. The cumulative strains at end systole of the non-infarcted (a) and infarcted (b) myocardia.

Preliminary statistical results from nine normal mice and seven infarcted mice showed the peak cumulative strains (i.e., total deformation during systole) were equal to 0.56±0.13 and -0.04±0.32, respectively.

IV. Conclusion and Discussion

In this paper, a high-resolution ultrasound system and a high frame rate acquisition system based on ECG triggering were used to acquire the RF signals of mice hearts. With a synchronization technique based on ECG triggering, an extremely high frame rate (up to 8000 frames / s) RF images was acquired. Incremental and cumulative axial displacement and elastograms as well as profiles of normal and infarcted mice myocardia indicated lower motion and deformation in the one-day old infarcted myocardium.

Calculation of cumulative displacement and strain helps improve the quality of displacement and strain estimation. In addition, the cumulative displacement and strain are less dependent on the heart rate of the mice and the frame rate of the system, and therefore provide a reliable measurement of the myocardium motion and deformation. Cumulative strains offered the highest contrast between non-infarcted and infarcted myocardia. Preliminary statistical results from nine non-infarcted mice and seven infarcted mice indicated myocardial elastography is feasible in assessing myocardial function and detecting early myocardial infarction *in vivo*.

Further studies also include the lateral displacements / strains estimation [11], which may provide additional information for assessing the myocardial function. Finally, recent angle-independent methods [12] could potentially be used for strain imaging with respect to the left-ventricular geometry.

Acknowledgment

The authors wish to thank Shunichi Homma, M. D., and Iwao Matsunaga, M. D., both with Columbia University, for kindly lending the ultrasound system used for the experiments presented here, and doing the mouse infarcts and operations, respectively.

References

[1] R. B. Willenheimer, L. R. Erhardt, C. M. J. Cline, E. R. Rydberg, and B. A. Israelsson, "Prognostic significance of changes in left ventricular systolic function in elderly patients with congestive heart failure," *Coronary Artery Dis.*, vol. 8, pp. 711-717, 1997.

[2] W. N. McDicken, G. R. Sutherland, C. M. Moran, and L. N. Gordon, " Colour doppler velocity imaging of the myocardium," *Ultrasound Med. Biol.*, vol. 18, pp. 651-654, 1992.

[3] A. Heimdal, A. Stoylen, H. Torp, and T. Skjaerpe, "Real-time strain rate imaging of the left ventricle by ultrasound," *J. Am. Soc. Echocardiogr.*, vol. 11, pp. 1013-1019, 1998.

[4] J. Declerck, T. S. Denney, C. Ozturk, W. O'Dell, and E. R. McVeigh, "Left ventricular motion reconstruction from planar tagged MR images: a comparison," *Phys. Med. Biol.*, vol. 45, pp. 1611-1632, 2000.

[5] J. Ophir, I. Cespedes, H. Ponnekanti, Y. Yazdi, and X. Li, "Elastography: A quantitative method for imaging the elasticity of biological tissues," *Ultrason. Imaging*, vol. 13, pp. 111-134, 1991.

[6] E. E. Konofagou, J. D'hooge, and J. Ophir, "Myocardial elastography - A feasibility study *in vivo*," *Ultrasound Med. Biol.*, vol. 28, pp. 475-482, 2002.

[7] S. Langeland, J. D'hooge, T. Claessens, P. Claus, P. Verdonck, P. Suetens, G. R. Sutherland, and B. Bijnens, "RF-based two-dimensional cardiac strain estimation: A validation study in a tissue-mimicking phantom," *IEEE Trans. Ultrason. Ferroelectr. Freq. Control*, vol. 51, pp. 1537-1546, 2004.

[8] J. D'Hooge, B. Bijnens, J. Thoen, F. Van de Werf, G. R. Sutherland, and P. Suetens, "Echocardiographic strain and strain-rate imaging: A new tool to study regional myocardial function," *IEEE Trans. Med. Imaging*, vol. 21, pp. 1022-1030, 2002.

[9] E. E. Konofagou, T. Harrigan, and S. Solomon, "Assessment of regional myocardial strain using cardiac elastography: Distinguishing infarcted from non-infarcted myocardium," *IEEE Ultrasonics Symp. Proc.*, 1589-1592, 2001.

[10] E. E. Konofagou, W. Manning, K. Kissinger, and S. D. Solomon, "Myocardial elastography: Comparison to results using MR cardiac tagging," *IEEE Ultrasonics Symp. Proc.*, 130-133, 2003.

[11] E. E. Konofagou, W. N. Lee, and C. M. Ingrassia, "A theoretical model for myocardial elastography and its *in vivo* validation," 27th Annual Conference of the IEEE Engineering in Medicine and Biology Society, Shanghai, China, Sept. 1-4, 2005.

[12] S. D. Fung-Kee-Fung, W. N. Lee, C. M. Ingrassia, K. D. Costa, and E. E. Konofagou, "Angle-independent strain mapping in myocardial elastography 2D strain tensor characterization and principal component imaging," *IEEE Ultrasonics Symp. Proc.*, 516-519, 2005.

[13] M. Pernot and E. E. Konofagou, "Electromechanical imaging of the myocardium at normal and pathological states," *IEEE Ultrasonics Symp. Proc.*, 1091-1094, 2005.